

GEOLOGIC REMOTE SENSING STUDY
OF THE
HAYDEN PASS - ORIENT MINE AREA,
NORTHERN SANGRE DE CRISTO MOUNTAINS, COLORADO

By

Daniel C. Wychgram

Remote Sensing Report 72-3

(NASA-CR-129519) GEOLOGIC REMOTE SENSING	N73-12385
STUDY OF THE HAYDEN PASS-ORIENT MINE AREA,	
NORTHERN SANGRE DE CRISTO MOUNTAINS,	
COLORADO D.C. Wychgram (Colorado School of	Unclas
Mines) Apr. 1972 68 p	CSCL 08G G3/13 16731

April 1972

GEOLOGIC REMOTE SENSING STUDY
OF THE
HAYDEN PASS - ORIENT MINE AREA,
NORTHERN SANGRE DE CRISTO MOUNTAINS, COLORADO

By


Daniel C. Wychgram

Remote Sensing Report 72-3

Bonanza Remote Sensing Project
Department of Geology
Colorado School of Mines
Golden, Colorado

NASA Grant NGL 06-001-015

Approved for Publication:


Keenan Lee
Associate Principal Investigator

April 1972

ABSTRACT

The Hayden Pass--Orient Mine area includes 60 square miles of the northern Sangre de Cristo Mountains and San Luis Valley in south-central Colorado. The rocks of this area include Precambrian igneous and metamorphic rocks, Paleozoic sedimentary rocks, Tertiary intrusive rocks, and Quaternary deposits.

Remote sensor data from a NASA Convair 990 radar flight and Mission 101 and 105 have been interpreted and evaluated. Based on interpretation of the remote sensor data, a geologic map (Plate II) has been prepared and compared with a second geologic map (Plate I), prepared from interpretation of both remote sensor data and field data. Comparison of the two maps gives one indication of the usefulness and reliability of the remote sensor data.

The usefulness and reliability of the remote sensor data are a function of the type of terrain as well as the type of remote sensor used. The San Luis Valley, with low relief and sparse vegetation, proved to be the best area to apply remote sensing. The western slope of the mountains is less suitable to the use of remote sensing techniques because of the dense coniferous cover and high relief. The eastern slope of the mountains, which is very densely covered with conifers and has high relief, is least suited to the use of remote sensing.

By using remote sensing as an aid in mapping the geologic features of the area, advantages were realized over purely field methods. These advantages include time savings, a greater understanding of

certain geological phenomena, and the compilation of a more accurate and complete geologic map.

Color and color infrared photography provided the largest amount of valuable information. Multiband photography was of lesser value and side-looking radar imagery provided no new information that was not available on small-scale photography. Thermal scanner imagery proved to be a very specialized remote sensing tool that should be applied to areas of low relief and sparse vegetation where geologic features produce known or suspected thermal contrast. Low sun-angle photography may be a good alternative to side-looking radar imagery but must be flown with critical timing.

CONTENTS

	Page
Abstract	ii
Introduction	1
Location and Physiography	1
Purpose	3
Acknowledgments	4
Description of Test Site	5
San Luis Valley--Area 'A'	5
West Flank of the Sangre de Cristo Mountains--Area 'B'.	8
East Flank of the Sangre de Cristo Mountains--Area 'C'.	11
Data Collection.	12
NASA Convair 990 Radar Flight	12
NASA Mission 101.	13
NASA Mission 105.	13
Interpretation and Evaluation of Remote Sensor Data.	18
Schedule and Method	18
Convair 990 Radar Flight.	20
Mission 101	22
Mission 105	27
Recent Supplementary Data--Mission 168	39
Conclusions.	46
Bibliography	53
Distribution	60

ILLUSTRATIONS

Figure	Page
1. Index map of Hayden Pass--Orient Mine area	2
2. Eroded fault scarp in the San Luis Valley.	7
3. Hypothetical cross section of a typical fault in the San Luis Valley.	9
4. Reproduction of Venus Fly-by radar imagery	21
5a. Annotated reproduction of Mission 101 color photography.	24
5b. Unannotated reproduction of Mission 101 color photography.	24
6. Geologic map based on interpretation of Mission 101 color and color IR photography	26
7a. Annotated reproduction of Mission 105 color photography.	28
7b. Unannotated reproduction of Mission 105 color photography.	28
8a. Annotated reproduction of RS-14 thermal infrared scanner imagery.	37
8b. Unannotated reproduction of RS-14 thermal infrared scanner imagery.	37
9a. Low sun-angle photography of fault scarps in San Luis Valley.	42
9b. Low sun-angle photography of fault scarps in San Luis Valley taken 16 minutes after Figure 9a.. . .	42
10. Forest Service photograph showing location of temperature monitoring stations.	44
11. Reproduction of Mission 168 thermal infrared imagery .	44

PLATES

Plate	Page
I. Geologic map and cross sections, Hayden Pass--Orient Mine area, Saguache, Custer, and Fremont Counties, Colorado	In Pocket
II. Geologic map based on remote sensor data--Map A; Map showing division of area into three subareas--Map B.	In Pocket

TABLES

Table	
1. NASA Convair 990 radar flight--flown May 19, 1969. . .	12
2. NASA Mission 101--flown August 11-12, 1969	14
3. NASA Mission 105--flown October 2, 1969.	15
4. Formational characteristics of Paleozoic and Precambrian rocks of area 'B' that are apparent on Mission 105 color photography	33
5. Summary of remote sensing instrument and data parameters--Mission 168.	40
6. Measurements on fault scarps in the San Luis Valley, June 16, 1971.	45

INTRODUCTION

This report is a summary of Master of Science thesis research activities performed from February 1970 through November 1971. Thesis research consisted of two parts; (1) description and interpretation of the stratigraphy, structure, and geologic history of the Hayden Pass--Orient Mine area, and (2) research into the application of remote sensor data to the geologic problems of this same area. In this report, the first part of the thesis is mentioned briefly and the second part, concerning geologic remote sensing, is discussed in detail. The reader is referred to the thesis (Wychgram, 1972), which is available at the Colorado School of Mines Library, for a detailed description of the geology of the area.

Location and Physiography

The Hayden Pass--Orient Mine area is in the rugged northern Sangre de Cristo Mountains, 25 miles southeast of Salida, Colorado (Figure 1). The area mapped includes approximately 60 square miles, extending from San Luis Creek on the southwest to the Arkansas River on the northeast, and from Hayden Pass Road on the northwest to the Big Cottonwood Creek and Black Canyon drainage systems on the southeast. The area includes parts of Rio Grande National Forest and Saguache County on the west side of the range crest and parts of San Isabel National Forest, Custer and Fremont counties, on the east side of the crest.

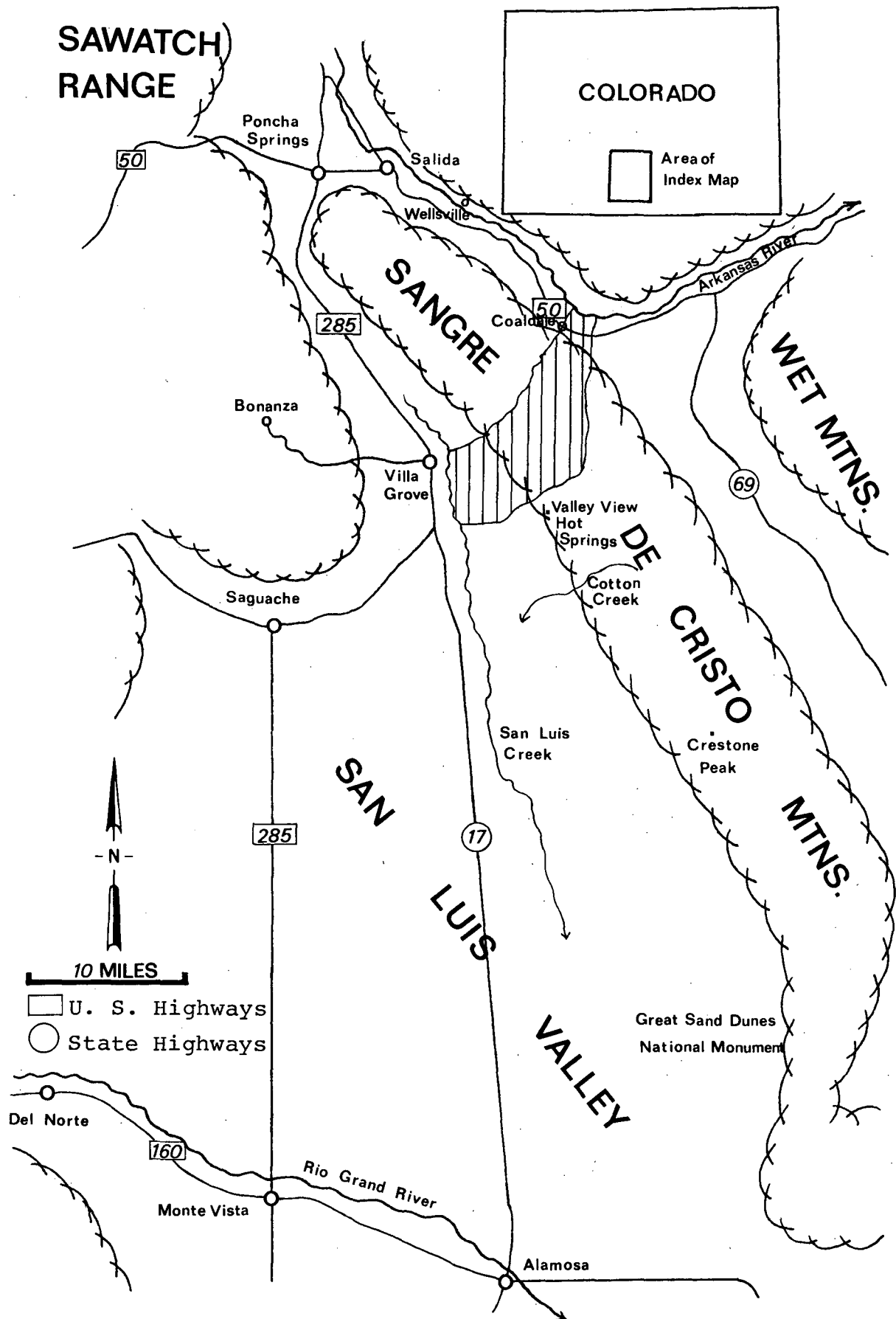


Figure 1. Index map of Hayden Pass--Orient Mine area (lined).

The Sangre de Cristo Range, one of the most spectacular ranges in Colorado, is characterized by its narrow width, high relief, and asymmetry. The peaks along the crest average more than 12,000 feet in elevation, and the relief between the Arkansas River at Coaldale and Nipple Mountain (12,199 feet) is almost 6,000 feet. The width of the range from the crest to its base in the San Luis Valley is only about 2 miles, whereas the width from the crest to the Arkansas River valley is about 6 miles. The sharply defined crest of the range, most of which is above timberline, is modified by alpine glacial features. The east side of the range is drained by tributaries of the Arkansas River. On the west side of the range, most of the runoff sinks into alluvial fans of the San Luis Valley near the base of the mountains.

Purpose

The area between Hayden Pass Road and the Orient Mine represented one of the last links in a chain of detailed geologic maps in the northern Sangre de Cristo Range. A purpose of this study was to contribute to the completion of this chain of detailed mapping.

A second purpose of the study was to interpret and to evaluate Bonanza Project remote sensor data and to determine the potential of the various remote sensor systems as applied to geologic problems. The Bonanza Project test site includes the northern Sangre de Cristo Range, and a limited amount of remote sensor data on the Hayden Pass--Orient Mine area was already available (see Tables 2, 3, and 4). The thesis area is particularly well suited to the evaluation of remote sensor data because it encompasses two markedly different

terrains, which provide remote sensor target variations concerning geology, hydrology, vegetation, and topography.

Acknowledgments

I am indebted to the Bonanza Remote Sensing Project, sponsored by the National Aeronautics and Space Administration (Grant NGL 06-001-015), which has provided financial support in the form of a Research Assistantship from February 1970 through August 1971 and the remote sensor data upon which much of this report is based. Furthermore, experience and knowledge gained in the planning and ground control activities of remote sensing missions and in course work related to the Project have greatly enhanced my ability to interpret the data used in this report.

Appreciation is expressed to the people of Martin Marietta Corporation's Interplanetary Geology Lab, especially to Messrs. Jim Muhm, Ken Worman, Roland Hulstrom, and Bob Biniki for help and advice.

I wish to thank Professors Keenan Lee, L. Trowbridge Grose, and Richard H. De Voto for advice and constructive criticism during field trips and meetings.

Finally, I wish to express sincere thanks to my wife, Virginia, for working with me for months in both the field and office as field assistant and secretary.

DESCRIPTION OF THE TEST SITE

Shortly after the Hayden Pass--Orient Mine area had been selected as the test site area, it was divided into three subareas. This division was based on natural topographic boundaries and the estimated relative degree to which remote sensing methods might be successfully applied to each subarea (Map 'B'--Plate II). This subdivision was made after a cursory appraisal of available remote sensor data.

San Luis Valley--Area 'A'

Area 'A' extends from San Luis Creek to the base of the Sangre de Cristo Mountains between Hayden Pass Road and the Orient Mine (Map 'B'--Plate II). This area includes all of the San Luis Valley that is situated within the thesis area and comprises about 20 square miles. The surface of the valley is covered by alluvial fan material derived from the mountains and by fluvial deposits associated with San Luis Creek.

The coalescing alluvial fans represent episodes of fan progradation with subsequent erosion and replacement by younger fans. A classification has been developed by Knepper (1972) which subdivides the alluvial fans into groups which have similar ages. By using remote sensor data, four groups of fans were easily mapped. It was found that alluvial fans of similar ages have characteristic geomorphology and vegetation associations. These features are discussed

by Wychgram (1972, p. 42-43) and under the heading "Interpretation and Evaluation of Remote Sensor Data" (p. 18).

The alluvial fans are cut by northwest trending faults which form fault scarplets up to 8 feet high (Figure 2). Most of these scarps face southwest, but three fault segments with scarps facing northeast were mapped in sections 20 and 21, T. 46 N., R. 10 E. The relative movement on these three fault segments is down on the northeast, whereas the relative movement on the other faults in the valley is down on the southwest. A normal fault of large magnitude, the Sangre de Cristo fault, separates the San Luis Valley from the Sangre de Cristo Mountains. Although covered by alluvial fan material throughout most of its length, the fault trace is expressed by alignment of vegetation near Oak Springs and by offset of fan material near the base of Steel Canyon.

Most of the water that flows from the canyons of the mountains sinks into the porous and permeable fan material of the valley. The vegetation in the valley is dominated by a sparse cover of grasses and cacti which reflect the semi-arid conditions (annual rainfall averages 10 to 15 inches per year). Limited shrub growth (mostly the greasewood, Sarcobatus vermiculatus, and rabbitbrush, Chrysothamnus ssp), is restricted to areas of relatively greater soil moisture close to the base of the mountains and along the few stream courses which manage to transport water over the alluvial-fan material. An exception to this pattern of shrub distribution occurs in the vicinity of sections 16, 17, 20, and 21, T. 46 N., R. 10 E. (Plate I), where the moisture is fault controlled. Apparently, the fault planes



Figure 2. Eroded fault scarp in San Luis Valley.
Dashed line marks base of scarp.

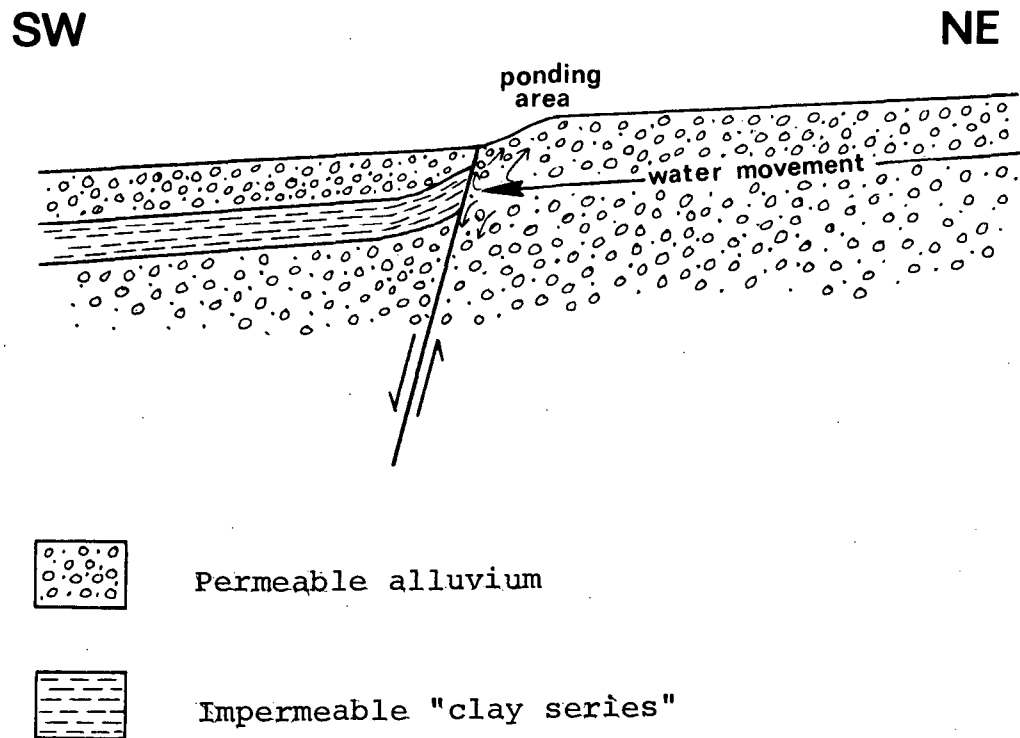
present a relatively impermeable barrier to ground water moving through the alluvial fan material from the mountain front to San Luis Creek. The mechanism of water impedance is not known for certain. Since the fault scarps in this area face southwest, the barrier cannot be topographic. A "clay series" (Powell, 1958), which usually occurs at depths of 50 to 130 feet, has been reported from water wells drilled in the vicinity. It is probable that one of these impermeable clay layers has been juxtaposed against permeable gravels on the northeast side of the fault (see Figure 3).

Area 'A' is considered to be the best subarea within the thesis area for successful application of remote sensing techniques.

West Flank of the Sangre de Cristo Mountains--Area 'B'

Area 'B' extends from the western base of the Sangre de Cristo Mountains to the crest of the range between Hayden Pass Road and Black Canyon (Map 'B'--Plate II). This rugged area has 3,700 feet of relief and includes approximately 18 square miles.

The rocks found in Area 'B' consist of Precambrian crystalline rocks and Paleozoic sedimentary rocks. The Precambrian rocks are exposed in a strip along the western-most side of the mountains which averages about half a mile wide. The Precambrian lithologies include meta-sedimentary rocks and scattered igneous intrusions. Locally, foliation is so well developed that it is often mistaken for stratification on aerial photographs. A sequence of lower and middle Paleozoic sedimentary rocks nonconformably overlies the Precambrian rocks and consists of relatively thin units of limestone, dolomite, and quartzite. Because of the high degree of resistance to erosion



Scale: none

Figure 3. Hypothetical cross section of a typical fault in the San Luis Valley (Area 'A') that restricts movement of ground water and results in ponding at the surface.

that is characteristic of these units, they are relatively well exposed. The contrasting lithologies of adjacent formations provide variations in color, vegetation, and geomorphology which facilitates discrimination and identification by remote sensing methods. Unconformably overlying the lower and middle Paleozoic rocks is a very thick sequence of upper Paleozoic clastic rocks. Some color contrast is provided by the lithologies occurring in the lower part of this sequence, but the similarities in gross lithology make differentiation of these units difficult. Only a fraction of the total upper Paleozoic section is present in Area 'B'. The rocks on the west side of the range are complexly folded and faulted.

The vegetation of Area 'B' is dominated by a thick cover of conifers. Two zones of coniferous trees are present that grade vertically into one another. The lower ponderosa pine--Douglas fir zone extends from the base of the mountains to about 9,500 feet. The spruce--fir zone extends upward from the vague upper boundary of the ponderosa pine--Douglas fir zone to timberline (approximately 11,500 feet). North-facing slopes support considerably denser stands of trees than south-facing slopes. In the valleys, and other areas of increased soil moisture, stands of aspen are present. Triangular faceted spurs along the western base of the range, and some south-facing slopes, support scrub oak and grass. Above timberline only grasses and a few dwarfed trees exist.

Area 'B' is considered to be a moderately well suited subarea within the thesis area for successful application of remote sensing techniques.

East Flank of the Sangre de Cristo Mountains--Area 'C'

Area 'C' extends from the crest of the range to the Arkansas River between Hayden Pass Road and Big Cottonwood Creek (Map 'B'--Plate II). The area includes approximately 23 square miles of rugged terrain. Relief is on the order of 6,000 feet.

Most of Area 'C' is underlain by upper Paleozoic sedimentary rocks. In general, the lithology of these rocks is mixed conglomerates, sandstones, siltstones, and shales. Formational boundaries are based largely on differences in color. Tertiary intrusive rocks occur as dikes along the crest of the range and as a stock-like intrusion in the vicinity of Slide Rock Mountain. Near the Arkansas River, Quaternary pediment gravels and alluvium cover the surface.

Most of the sedimentary rocks of Area 'C' are folded in a regular manner. An important set of northwest trending faults were detected on small scale photography. Field evidence in support of these structures is often minimal. It appears that three of these faults may have been significant to the emplacement of the Slide Rock Mountain Intrusive (see Plate I).

Area 'C' supports a very dense forest of conifers. The same vertical zonation of tree types exists as in Area 'B'. Because of the high density of coniferous growth, rocks are rarely seen on aerial photographs. Some of the southern facing slopes are relatively free of conifers but are usually well covered by scrub oak. A few deciduous trees grow in the lower areas near the Arkansas River. Many areas underlain by pediment gravels or alluvium are cultivated.

Of the three subareas discussed, Area 'C' is considered the least satisfactory for successful application of remote sensing methods.

DATA COLLECTION

Variables involved with the collection of remote sensor data are discussed in this section. A table is presented for each data-producing mission that summarizes important system and data parameters. Only data that concern the thesis area are considered.

Table 1. NASA Convair 990 Radar Flight--Flown May 19, 1969

<u>Mode</u>	<u>System</u>	<u>Freq.</u>	<u>Format</u>	<u>Scale</u> <u>(approx.)</u>	<u>Coverage</u>	<u>General</u> <u>Quality</u>
SLAR	Venus Fly-by	1.2 GHz	5" wide prints	1:87,000 to 1:118,000	Most of thesis area	Fair

NASA Convair 990 Radar Flight

Table 1 summarizes parameters of the Venus Fly-by radar data. Two lines of side-looking radar were flown by the NASA-Ames Convair 990 aircraft. The coverage was obtained as part of a test for the Venus Fly-by radar system. The system's 1.2 GHz center frequency provides a relatively long wavelength of 25 cm. The two northwest trending strips were flown at an altitude of 29,000 feet. The western-most strip 'looks' east at portions of the San Luis Valley and Sangre de Cristo Mountains starting from Black Canyon and continuing into the Upper Arkansas Valley. Average scale of this slant range imagery is: range scale, 1:97,500; azimuth scale, 1:87,000. The eastern strip looks west and covers portions of the Sangre de Cristo range north of Cottonwood Creek. The average scale for this strip is: range scale, 1:95,000; azimuth scale, 1:118,000. The geometric quality of the imagery, as reflected by differences in azimuth and range scales, is better on the western strip. The resolution of this radar imagery is very coarse.

NASA Mission 101

Mission 101 was flown at approximately 60,000 feet above sea level using a NASA RB-57 aircraft. Table 2 summarizes parameters of Mission 101 data. Color, color IR, and three bands of multiband photography were obtained. Stereo color transparencies (and black and white prints made from the transparencies) were obtained from an RC-8 camera with 6-inch focal length lens. An identical camera, triggered synchronously, was used to get comparative stereo color IR transparencies. A third camera, a Zeiss RMK A 30/23 with 12-inch focal length lens, was also used with color IR film. Since the scale of the Zeiss photography was twice as large as the RC-8 photography, stereo coverage was not obtained with this camera.

Multiband photography was obtained with three Hasselblad 70mm cameras equipped with 3-inch focal length lenses. All three cameras were tripped simultaneously to give comparable frame coverage. The resulting photography is of extremely small scale. The 700-900nm bandpass is seriously degraded by static discharge marks and streaking. Cloud loss is significant in several frames.

NASA Mission 105

The NASA 927-NP3A aircraft, flying at 17,500 and 25,000 feet above sea level, was used for Mission 105. Table 3 summarizes the parameters of Mission 105 data. Only a

Table 2. NASA Mission 101--Flown August 11-12, 1969

<u>Mode</u>	<u>System</u>	<u>Bandwidth</u>	<u>Film Filter</u>	<u>Format</u>	<u>Scale (Approx.)</u>	<u>Coverage</u>	<u>General Quality</u>
Photography	Wilde RC-8	400-700nm	2448	9"x9" (T) & B/W(P)	1:100,000	Entire thesis area	Excellent (few clouds)
Photography	Wilde RC-8	520-900nm	SO-117 W-15	9"x9" (T)	1:100,000	Entire thesis area	Excellent (few clouds)
Photography	Zeiss RMK A 30/23	500-900nm (approx.)	SO-117 Zeiss 'B'	9"x9" (T)	1:50,000	Most of area except just east of mtn. crest	Excellent (few clouds)
Photography (Multiband)	Hasselblad	480-590nm	2402 W-57	70mm (T)	1:200,000	All of Area 'A', parts of Areas 'B' & 'C'	Fair
Photography (Multiband)	Hasselblad	590-700nm	2402 W-25A	70mm (T)	1:200,000	All of Area 'A', parts of Areas 'B' & 'C'	Fair to Good
Photography (Multiband)	Hasselblad	700-900nm	SO-246 W-89B	70mm (T)	1:200,000	All of Area 'A', parts of Areas 'B' & 'C'	Poor

NOTE: Photography bandwidths calculated by using the 10 percent transmittance value point on Wratten filters and assuming that the responses of 2402 film and SO-246 film extend to 700nm and 900nm respectively. W = Wratten; (T) = Transparencies; (P) = Prints

Table 3. NASA Mission 105--Flown October 2, 1969.

<u>Mode</u>	<u>System</u>	<u>Bandwidth (or Freq.)</u>	<u>Film Filter</u>	<u>Format</u>	<u>Scale (Approx.)</u>	<u>Coverage</u>	<u>General Quality</u>
Photography (Color)	Wilde RC-8	400-700nm	SO-397 Anti-Vignetting	9"x9" (T&P)	1:15,000	Area 'A'; Parts of Area 'B'	Good
Photography (Color IR)	Wilde RC-8	520-900nm	SO-117 W-15 CC-20M 4600	9"x9" (T)	1:15,000	Area 'A'; Parts of Area 'B'	Poor
Photography (Multiband)	KA-62A	A 590-700nm	2402 W-25A	5"x5" (T)	1:41,000	Area 'A'; Part of Area 'B' near base of range Small part of Area 'C'	Fair
Photography (Multiband)	KA-62B	B 400-470nm	2402 W-47B	5"x5" (T)	1:41,000	"	Fair
Photography (Multiband)	KA-62C	C 500-580nm	2402 W-58	5"x5" (T)	1:41,000	"	Fair
Photography (Multiband)	KA-62D	D 700-900nm	SO-246 W-89B	5"x5" (T)	1:41,000	"	Fair
IR Scanner	RS-14	3-5.5 μ m	NA	2.5" wide strip positive (T)	L36 1:46,000	All of Area 'A': Part of Area 'B' near base of range. Small part of Area 'C'	Fair to Good
IR Scanner	RS-14	8-14 μ m	NA	2.5" wide strip positive (T)	1:46,000	"	Good
SLAR	DPD-2	16.5 GHz	NA	2" wide strip positive (T)	1:300,000	Areas 'A' & 'B'	Very Poor
Multifrequency Microwave Radiometry	None Given	1.4 GHz 10.625 GHz 22.235 GHz 22.355 GHz 31.4 GHz	NA	Analog Magnetic Tape	NA	One line near base of moun- tains in San Luis Valley	Very Poor

NOTE: Photography bandwidths calculated by using the 10 percent transmittance value point on Wratten filters and assuming that the response of 2402 film and SO-246 film extends to 700nm and 900nm respectively. W = Wratten; (T) = Transparencies; (P) = Prints

fraction of Mission 105 objectives were accomplished due to poor weather and technical problems which resulted in unflown data lines and much unusable data.

Large scale color photography was obtained using an RC-8 camera fitted with an anti-vignetting filter. The resulting photography was of generally good quality except for some exposure problems. One side of the photographs tended to be darker than the other side. This differential darkening, which is more prominent in areas of high relief, is probably a function of the low sun angle which existed when the mission was flown. One line, which was flown in Area 'C', was too dark to use. This underexposure was probably the result of the very dense cover of conifers which have a low albedo. Stereo coverage is good in Area 'A' but marginal in Area 'B' and nonexistent in Area 'C'. The poor stereo viewing geometry is the result of severe crab used by the aircraft in order to counter strong crosswinds. The color IR has the same geometry problems and, in addition, is considerably underexposed. The color IR photography has an overall green color with some red occurring only where very abundant, healthy, nonconiferous vegetation was photographed. The color IR photography also suffers from vignetting and poor focus.

Four KA-62 cameras employing 3-inch focal length lenses were used to obtain multiband photography. The quality of the KA-62 photography was degraded by lack of good registration.

An RS-14 thermal IR scanner, recording in both the 3-5.5 μ m and 8-14 μ m bandwidths, was flown over Area 'A' and parts of Area 'B'. This imagery was obtained from about 12:11 hrs. to 13:10 hrs. Pre-dawn imagery could not be obtained due to poor weather conditions. Most of the transparencies, which were prepared from the magnetic tape output of the scanner by NASA, are of good quality. However, the 3-5.5 μ m band imagery is quite "liney" and some areas of coverage, particularly the mountainous regions, are underexposed. As received from NASA, much of the imagery was mislabeled as to which of the two channels produced it (see Lee, 1971, p. 14-15). Detracting somewhat from the comparative value of the two channels is the fact that they are not in register and are of slightly different scales.

Five lines of SLAR were flown on Mission 105. One line, which covers the west side of the northern Sangre de Cristo Range and parts of the San Luis Valley, involves the thesis area. This imagery is extremely noisy, has poor resolution, and is of very small scale. One line of multifrequency microwave radiometer data was obtained near the base of the mountains in the San Luis Valley. The data were very noisy, poorly calibrated, and lacked boresight camera reference data.

Before, during, and after the flying of Mission 105, geologists from Colorado School of Mines and Martin Marietta Corporation monitored surface and micrometeorological variables.

These variables included: cloud type and cover, wind speed and direction, relative humidity, air temperatures, radiometric (8-14 μ m and L-band) temperatures, and contact (thermister) temperatures. In addition, soil samples were collected and soil moisture content measured from these samples.

NASA Mission 115, scheduled for December 3, 1969, was postponed due to instrument malfunctions then cancelled because of adverse weather. Mission 153 (October 13-27, 1970) was also cancelled because of poor weather conditions, however, some photography was obtained outside the thesis area. Mission 168 (June 14-16, 1971) provided much useful data concerning the thesis area. These data are discussed on p. 39.

INTERPRETATION AND EVALUATION OF REMOTE SENSOR DATA

This section discusses research activities involved with the interpretation and evaluation of remote sensor data. The data are grouped according to the NASA mission that generated them. This section is introduced by a discussion of the schedule and methods used in evaluation of the data.

Schedule and Method

Dividing the thesis area into three subareas facilitated the integration of lab work and field work on a schedule that

would provide a more meaningful evaluation of remote sensor data. The general plan was to interpret the data, having little or no a priori knowledge of the area. First, a geologic map based on interpretation of the remote sensor data (Plate II) was prepared. Then a second map (Plate I) was prepared based on field observations in combination with the information available through remote sensing. Comparison of the two maps provides one indication of the usefulness and reliability of the remote sensor data.

Laboratory methods consisted of studying transparencies of the Missions 101 and 105 photography and imagery on a light table. Stereo viewing was employed where possible. The geologic interpretations were traced onto frosted mylar and then transposed to the base map using a variable scale projection technique.

The first subarea to be evaluated according to this sequence was Area 'C'. This was done because the least amount of remote sensor data was available of this area. This fact insured that interpretation could easily be completed before the 1970 summer field season began. Mission 101 color and color IR photography was studied, and several lineaments were mapped as possible faults. One line of Mission 105 photography was flown over Area 'C', but lack of stereo overlap and underexposure made these data worthless. During July and August of 1970, Area 'C' was field mapped and photogeologic features were field

checked. In preparation for the interpretation of remote sensor data of Area 'B', the formational contacts on the ridge between Silver Creek and North Piney Creek were also mapped.

During academic year 1970-71, Missions 101 and 105 remote sensor data were interpreted for Areas 'A' and 'B'. Color, color IR and multiband photography and thermal IR imagery were analyzed and geologic interpretations placed on a base map (Plate II). The previous field mapping done on the ridge between Silver Creek and North Piney Creek allowed the identification of formations and proper placement of contacts during this initial phase of mapping. Due to the complexity of structure in Area 'B' and the discontinuous exposure, considerable time was required to complete the interpretation. The alluvial fans and normal faults of the San Luis Valley, however, required less than a week of laboratory time to map. During July of 1971, subareas 'A' and 'B' were field checked and the map of Plate I was completed.

Convair 990 Radar Flight

The entire thesis area was imaged by the long wavelength, Venus Fly-by radar system. The resolution of this imagery is very coarse and only major topography is discernible. Parts of Areas 'A' and 'B', as imaged on the western-most strip of imagery, are shown in Figure 4. The break in topography between the San Luis Valley and the Sangre de Cristo Mountains

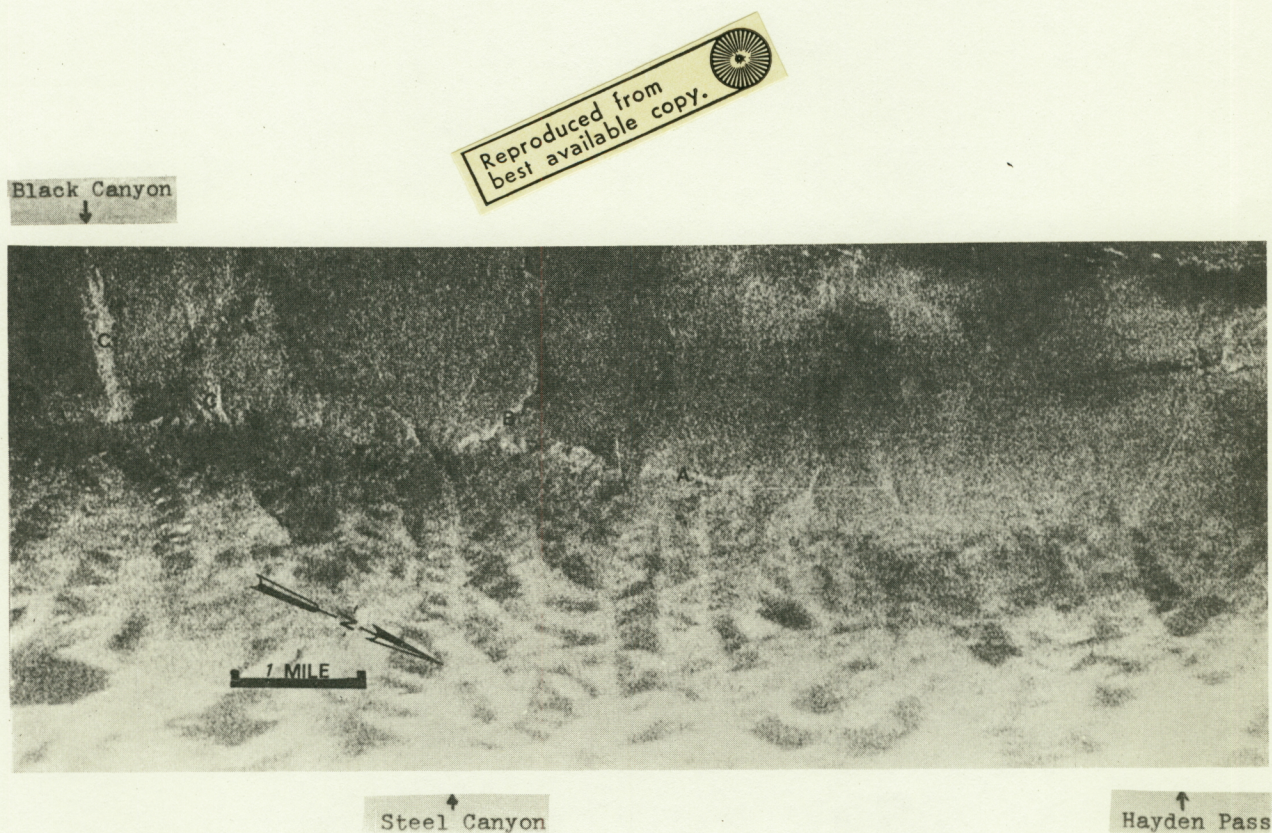


Figure 4. Reproduction of Venus Fly-by radar imagery. Radar system frequency is 1.2 GHz; look direction is to northeast; polarization is unknown.

is apparent (see feature A, Figure 4). A very high return was received from a south facing erosional scarp (approximately 50 feet high) developed in alluvial fan material northwest of Steel Canton (see feature B, Figure 4). Concentrations of shrub growth in the San Luis Valley are evident near the base of the mountains (see features C, Figure 4). The fault scarps of the San Luis Valley were not resolved by the system.

The eastern strip of imagery has lower contrast than the western strip. Even major topographic features are difficult to identify because of this low contrast.

No significant geologic data were contributed by the Convair 990 radar imagery. Radar imagery of this quality would be of very marginal value in even a more generalized regional study.

Mission 101

Mission 101 photography provided considerable aid in the selection of the Hayden Pass--Orient Mine area as a test site. The small scale (<1:100,000) allowed the viewing of large areas rapidly. In general, areas of igneous and metamorphic rock could be easily distinguished from areas of sedimentary rock. Since I was interested in working with sedimentary rocks, this helped narrow the search considerably.

Within the thesis area, rock discrimination was minimal.

In Area 'C', parts of the Tertiary intrusive could be discriminated from the surrounding sedimentary rocks (Figure 5). The small intrusive mapped in Pole Gulch on Plate I can be seen at the end of the arrow in Figure 5a. However, it was not recognized as such in the original interpretation. Precambrian terrain northeast of the Arkansas River and east of Big Cottonwood Creek was easily distinguished from the sedimentary rocks of the thesis area (Figure 5a). In Area 'B', the contact between Precambrian crystalline rocks and Paleozoic sedimentary rocks could not be accurately mapped on the small-scale photography. The strongly developed foliation of the Precambrian rocks and the thick growth of conifers contributed to this poor discrimination. The lower and middle Paleozoic rocks were easily recognized as sedimentary rocks but discrimination or identification of the thin formations was impractical with photography of such small scale. Accurate differentiation of the alluvial fans of the San Luis Valley was not possible, but some individual fans could be recognized and variations in drainage density were noticeable.

Considerable structural information was available on the Mission 101 photography. The normal faults of Area 'A' were very apparent where ponding had occurred. Some of the fault scarps could be faintly seen and mapped under high magnification. The larger folds and faults of Area 'B' were first mapped on small scale color photography. Parts of the

Reproduced from
best available copy.

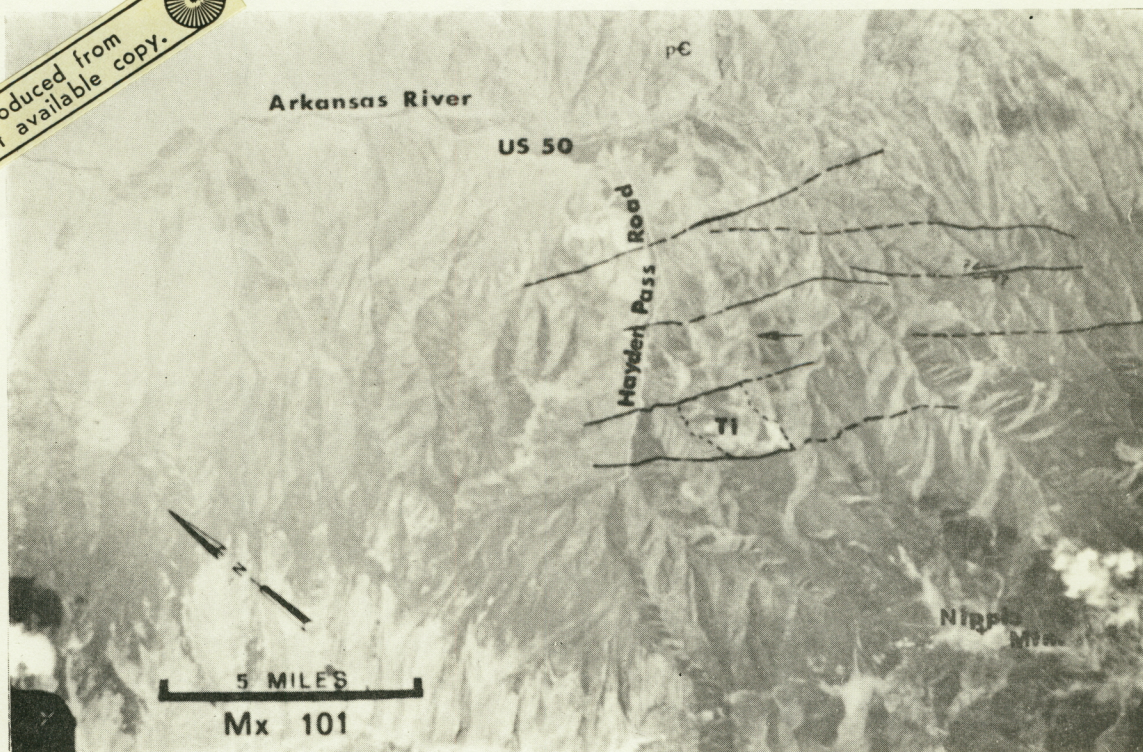


Figure 5a. Annotated reproduction of Mission 101 color photograph. Area 'C' shown.



Figure 5b. Unannotated reproduction of Mission 101 color photograph. Same coverage as Figure 5a.

Steel Canyon anticline and syncline, and offsets related to the Silver Creek fault, were detected (see Figure 6). The most significant structural information gleaned from Mission 101 photography was the detection and location of several northwest-trending lineaments in Area 'C' (Figure 5). These lineaments are primarily expressed topographically where small and medium scale drainage is aligned along linear trends. In some areas, these lineaments are enhanced by vegetation contrast across the lineament. In all cases, except next to the Tertiary intrusive, this vegetation contrast seems to be controlled by topographic rather than lithologic control. Field evidence supports four of the five lineaments mapped from Mission 101 photography in Area 'C' (compare Plates I and II). It is significant to note that these lineaments are generally not detected on larger scale photography such as U. S. Forest Service (1:20,000 scale) black and white photography.

The difference in available information between the Mission 101 color and color IR photography is negligible. Both films did an equal job of rock discrimination. Since vegetation was significant in delineating faulting in Areas 'A' and 'C', color IR may be slightly superior in these areas. However, this advantage was judged insignificant to the final interpretation. It is interesting to note that the lineaments in Area 'C' were mapped with equal or greater ease, compared with color and color IR, on black and white contact

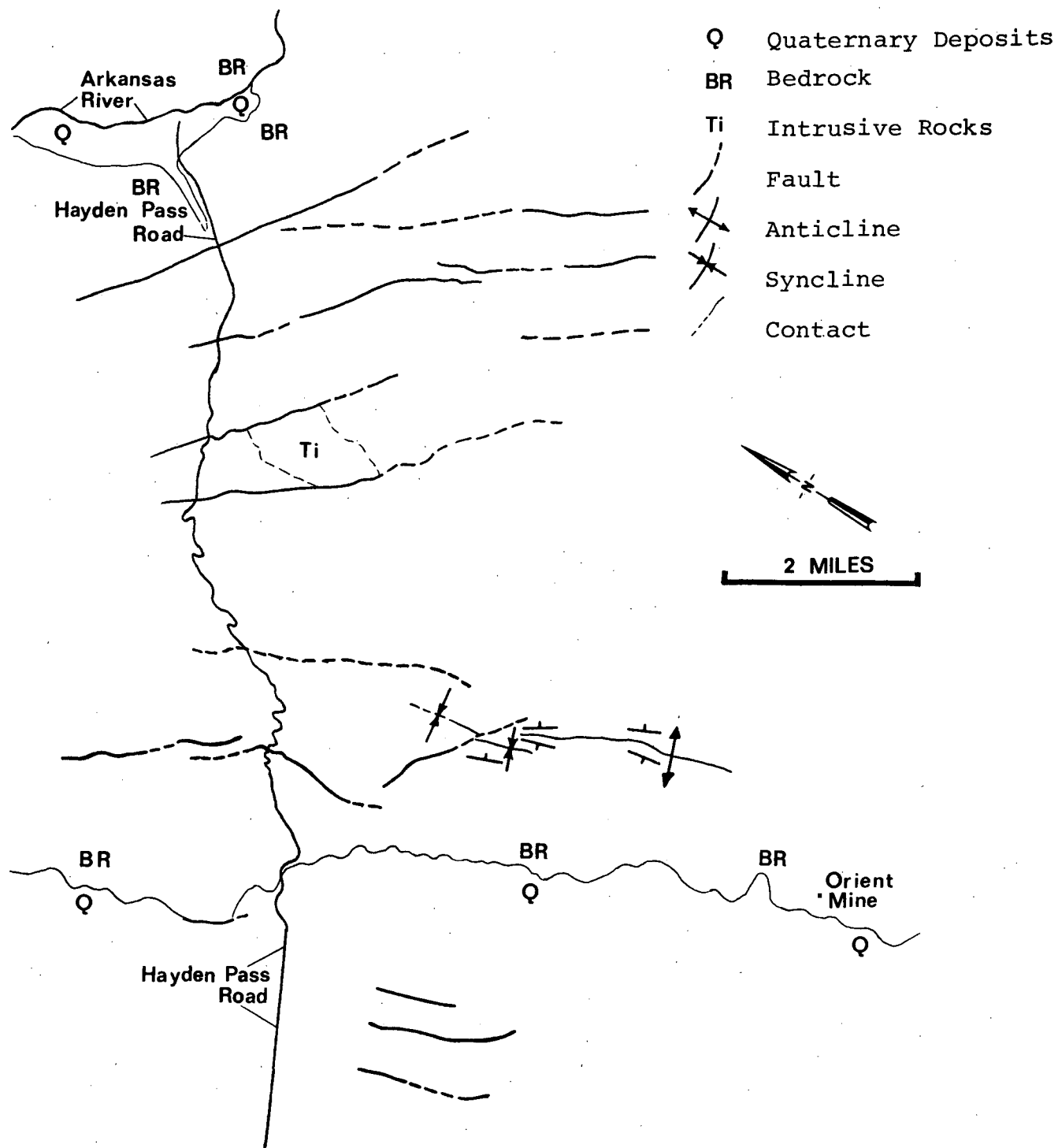


Figure 6. Geologic map based on interpretation of Mission 101 color and color IR photography.

prints made from the color transparencies. The reason for this seeming anomaly is not clear. The Zeiss color IR photography did not provide stereo viewing and was not studied in detail. However, it was obvious that some linear features, such as the fault traces of Area 'A', could be extended somewhat beyond what could be done with the Mission 101 RC-8 photography. This was entirely due to the more favorable scale and resolution of the Zeiss photography.

The multiband photography was of too small a scale to be used for anything but a more generalized regional study. Comparison of the three bandpasses is meaningless due to the high degree of variation in quality between the data. No additional information was available from the multiband photography that was not available on the color and color IR RC-8 photography.

Mission 105

The RC-8 color photography of Mission 105 was of large enough scale to provide for interpretation of detailed geology. Overall, this photography provided more useable geologic information than all the other modes of remote sensing combined. The geology of Areas 'A' and 'B' of Plate II was compiled based on interpretation of these data.

In Area 'A', the alluvial fans could be discriminated and identified. Figure 7 shows annotated and unannotated reproductions of Mission 105 color frame number 6252. On

Reproduced from
best available copy.

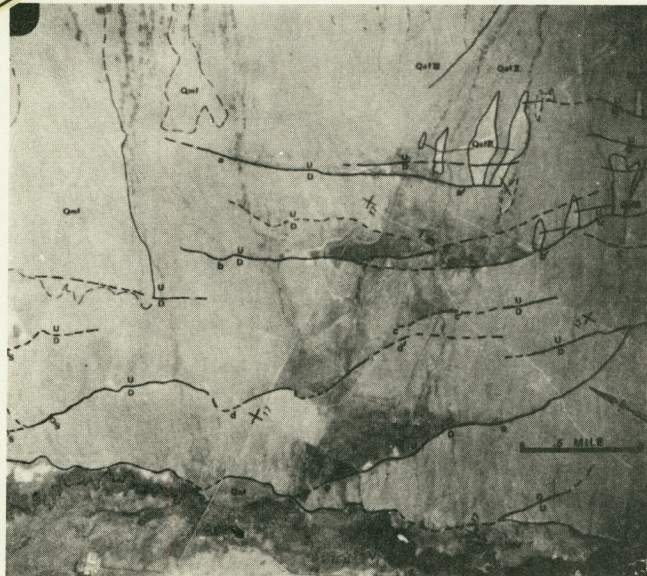


Figure 7a. Annotated reproduction of Mission 105 color photograph. Portion of Area 'A' shown. Qmf = mud flow; Qal = alluvium; Qaf II = fan Unit II; Qaf III = fan Unit III; Os = spring.

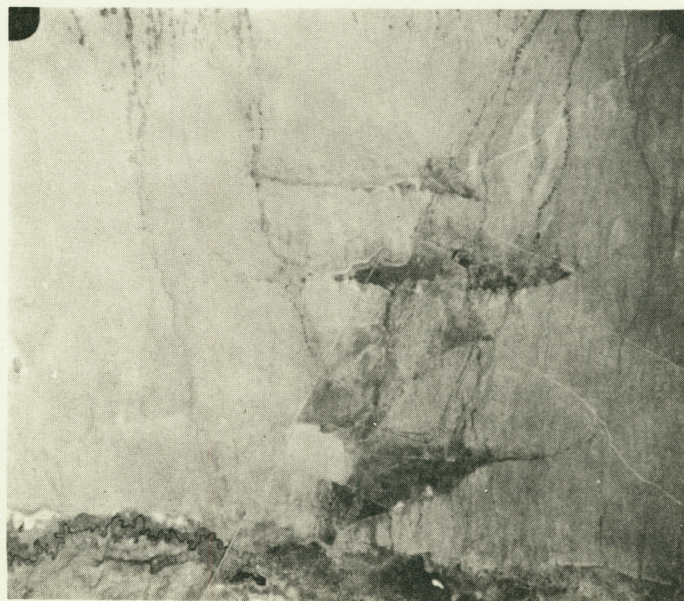


Figure 7b. Unannotated reproduction of Mission 105 color photograph. Same area as Figure 7a is shown.

it are representatives of two of the four alluvial fan groupings. The oldest fan unit shown, Qaf III, has a higher drainage density and is topographically higher than the younger fan unit, Qaf II. Also, note that Qaf III has a slightly higher density of shrub growth. This difference in vegetation density is more apparent near the base of the mountains. Although it may not be noticeable in Figure 7 without stereo viewing, the surface of Qaf II is more gently sloped than that of Qaf III. Small erosional remnants of fan unit Qaf III have been mapped that are surrounded by Qaf II (Figure 7). These remnants of fan unit Qaf III are recognized on the photography by lighter tones and higher elevation than the surrounding Qaf II material. When later observed in the field, a relief of over 10 feet was apparent between the surfaces of the old fan remnants and the surface of the surrounding younger fan. The lighter tone of the erosional remnant surfaces is a result of the winnowing of fine material from these higher areas. This process leaves coarser material, much of which is caliche covered, exposed at the surface. As further evidence of the age relationship of the two fan units, observe that the distributaries of fan Qaf III are truncated by Qaf II. Similar criteria, which can be observed on Mission 105 color photography, are used to differentiate, identify, and correlate the other fan units of Area 'A' (see also Wychgram, 1972, p. 42-43).

Another surface material unit has been differentiated in Figure 7 based on surface pattern and texture. This unit, designated Qmf, was interpreted to be a mud flow in which the material became supersaturated with water and flowed as a unit. The flow-like pattern of the surface strongly suggested this genesis. Field observations of these features, conducted during July of 1971, did not support this interpretation. The lighter colored areas are slightly higher than the darker areas and are covered with rock debris that is both caliche-covered and of generally light colored lithologies. In addition, these higher areas display a relatively sparse cover of grass. The anomalous pattern then, appears to be the result of the winnowing of fine material from the higher areas and the deposition of this material in the adjoining low areas. In addition to covering coarse rock debris in the lower areas, this fine material provides a more favorable substrate for grass.

Figure 7 also shows several of the fault traces of Area 'A' that are expressed as low relief scarps. The fault segments labeled a-a', b-b', c-c', d-d', and e-e' are impeding the flow of subsurface water that is moving from east to west (see discussion, p. 6-8 and Figure 3, p. 9. The resulting increase in relative soil moisture has caused an anomalously high density of vegetation on the east side of the faults. Although stereo viewing is necessary to accurately map the fault traces which are not damming

subsurface water, many of these features can be seen without the aid of stereo because of the differences in vegetation, soil, and lighting associated with the scarp slope.

Except for the postulated mud-flow features, field checks have supported all of the interpretations made in Area 'A' that were based on Mission 105 color photography. It was realized while making the field checks that compiling a geologic map of equal accuracy and completeness of Area 'A' by field mapping methods would be impractical, if not impossible.

In Area 'B', the large scale color photography is of lesser quality. The resolution of some frames is poorer and, because of dense stands of conifers, underexposure is common. The underexposure problem is amplified on north slopes because of low sun-angle and high relief. Excess aircraft yaw, used to compensate for cross winds during the overflight, resulted in a geometry which makes stereo viewing difficult. However, the large scale and good color rendition of the photography provided enough information to compile a fairly detailed geologic map of this area (see Plate II).

As previously mentioned, formational contacts were field mapped on the ridge between North Piney and Silver Creeks before laboratory interpretation began. This provided some familiarity with the lithologies and thicknesses of the formations. By later comparison of the field

mapped contacts with the color photographs, the signature characteristics of each formation and the formation boundaries were established. During interpretation, instead of merely discriminating different lithologic units and identifying these as shale, sandstone, limestone, etc., formational contacts and formational names could be applied.

The following table (Table 4) summarizes the formational characteristics that are evident on the color photography and are the basis for discrimination and identification of the rock units of Area 'B'.

Faults of Area 'B' were mapped largely on the basis of truncated or offset strata. It was noted that aspen often prefer to grow on fault zones (increased soil moisture?). The autumn photography displayed the aspen in high contrast with the conifers.

Comparison of Area 'B' on Plate I (field checked) and Plate II (interpretation of remote sensor data) reveals several discrepancies. The number of, and placement of, faults varies between the two maps, especially in the Steel Canyon area. In the vicinity of Steel Canyon, the rocks are complexly folded and faulted. The map of Plate I represents the best interpretation of data collected in the field in combination with information available from Mission 105 photography. Much more study of this area would be required to gain a full understanding of the complex structure.

Table 4. Formational characteristics of Paleozoic and Precambrian rocks of Area 'B' that are apparent on Mission 105 color photography.

Kerber Formation (Pk)	Less resistant; no outcrops, many trees.
Leadville Limestone (Ml)	Very resistant; high topography; light color; few trees; usually well exposed.
Chaffee Formation (Dc)	Characteristic yellow color; often tree covered; less resistant than Ml or Of. Contact between Dc and Of difficult to place--often based on thickness.
Fremont Dolomite (Of)	More resistant than Dc.
Harding Sandstone (Oh)	Very resistant; forms higher topography; fewer trees; notably stratified; source of many talus screens. Contact often covered by talus of Oh.
Manitou Dolomite (Om)	Less resistant than Oh; yellowish color, thickness important. Contact usually placed based on thickness of Om.
Precambrian (pE)	Similar resistance to Om; strong foliation but usually not at same attitude as bedding of adjacent sedimentary rocks, talus screens similar to Oh.

Two longitudinal faults (faults X and Y, Plate I), which start in Black Canyon and end in Steel Canyon, were only partly detectable on the color photography where strata were offset or terminated. In the field, placement of these faults is based largely on anomalous stratigraphic thickness. The transverse fault mapped between North and South Piney creeks was misplaced on its eastern end on Plate II. Field checking of this feature revealed that brecciation and subsequent silicification of the Kerber Formation (a quartzose sandstone) had made it much more resistant than it normally is. As a result, it appeared similar to the resistant Leadville Limestone on the color photography, which lead to the erroneous fault placement. In one area, on the ridge between Black and Lime canyons, so little geological information was available on the photography that it was left blank on Plate II.

The color IR photography of Mission 105 is of little value because of the overall greenish color. This is unfortunate, because the large scale of the photography would have made possible the detailed comparison of the relative usefulness of color and color IR films as applied to the geologic problems of the thesis area.

Mission 105 produced four bands of multiband photography. This photography is of adequate scale and quality to resolve many geologic features of the thesis area. The photography produced from all four film-filter combinations was examined

simultaneously on a light table. Lack of time prevented the use of more sophisticated methods of data enhancement, such as masking and color additive viewing. As is the case with Mission 101 multiband photography, it appears that no significant additional information is available from the multiband photography which is not available on the RC-8 color and color IR photography. It should be noted that the film-filter combinations used were not designed to discriminate the rocks of the thesis area. However, it was judged that Band 'D' (700-900nm) provides a better indication of the condition of grass and deciduous vegetation than did the color IR photography since Mission 105 color IR photography was improperly filtered. Marrs (Lee, 1971, p. 44-45), commenting on similar data involving the Bonanza Mining District, stated that variations in reflectance from conifers was exhibited on Bands 'B' and 'D' (400-470nm and 700-900nm respectively). Although this variation was not detected in the thesis area, more study of these two bands directed toward isolation of this spectral variance may be warranted. Variations in reflectance from conifers may be related to the geologic materials upon which the conifers grow.

The daytime thermal IR scanner imagery produced by Mission 105 is of good quality. In the mountainous areas, topography is well defined. The 3-5.5 μ m imagery, which is of higher contrast than the 8-14 μ m imagery, is locally

underexposed resulting in loss of all information. Barren areas (grass or dirt covered) can be easily distinguished from forested areas. Because of this discrimination ability, the imagery displays stratification of sedimentary rocks close to timberline (alternating vegetation zones), delineates most of Hayden Pass Road, and is able to discriminate parts of the resistant lower and middle Paleozoic rocks where these units are barren of vegetation. Neither of the igneous dikes that are exposed along the crest of the range are discriminated. The high contrast of the 3-5.5 μ m channel imagery is an advantage on a line of imagery along the base of the mountains (Line 35) where conifers are not the dominant vegetation. The alignment of trees near Oak Springs (on the trace of the Sangre de Cristo fault) and the distribution of shrub growth on the alluvial fans is well defined on this imagery. On the two lines of imagery that include the fault scarps of the San Luis Valley (Lines 33 and 34), the "lineyness" of the 3-5.5 μ m imagery degrades image resolution to such a degree that much detail of relative temperature distributions associated with the faulting is lost. The relatively high resolution provided by the 8-14 μ m imagery reveals interesting thermal details (Figure 8) of the ponding on the fault segment labeled a-a' on Figure 7a. The fault scarp itself is warm, but in the area of ponding, two relatively cool areas are surrounded by warmer areas. The cool spots are the result of both high soil moisture

Reproduced from
best available copy.

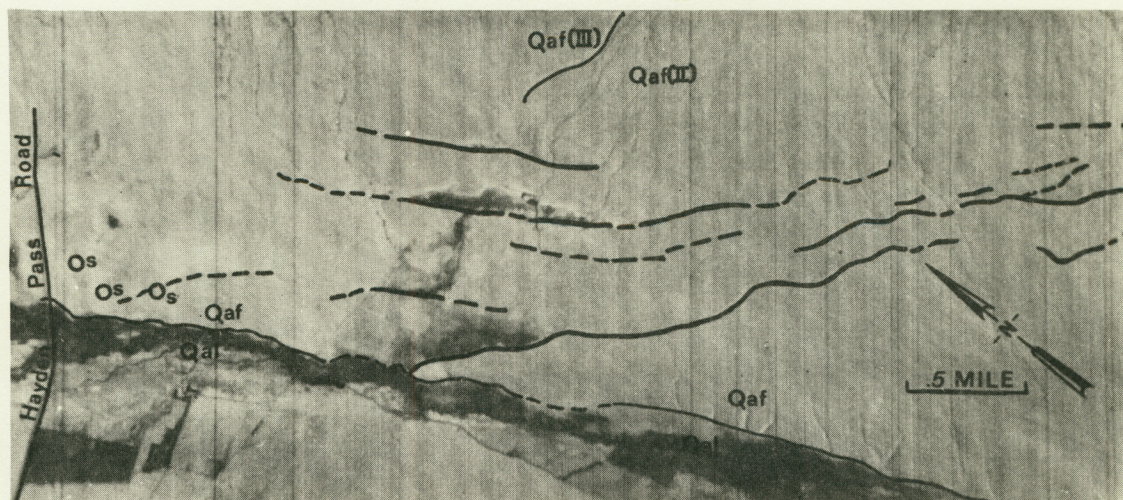


Figure 8a. Annotated reproduction of RS-14 thermal infrared scanner imagery (8-14 μ m). Qal = Quaternary alluvium; Qaf II = alluvial fan Unit II; Qaf III = alluvial fan Unit III; Os = spring. The area of ponding discussed on p. 105-106 is just below the line separating Qaf III from Qaf II at the top of the figure. Imagery taken at 1300 hours on October 2, 1969.

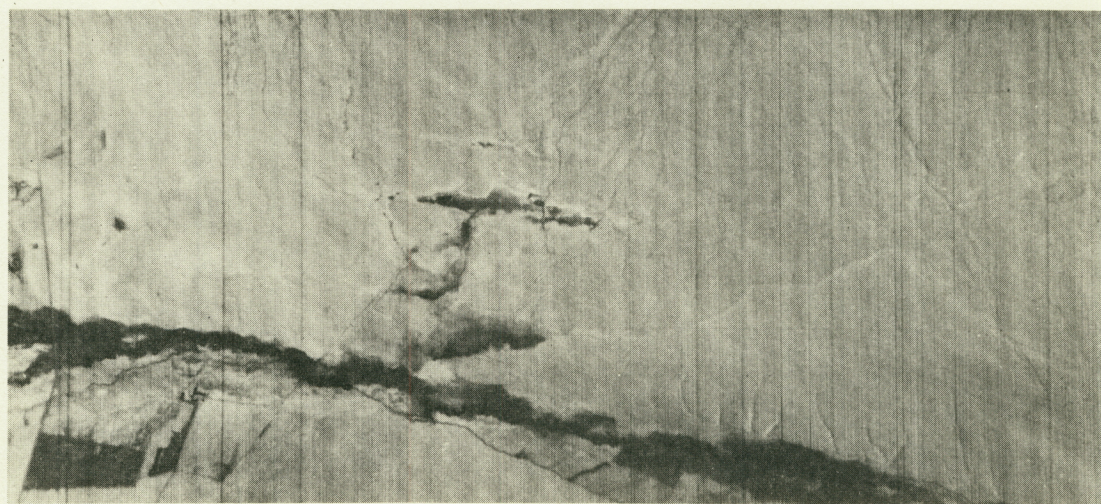


Figure 8b. Same as Figure 8a without annotations.

(evaporative cooling) and concentrations of vegetation. The relatively warm area surrounding the cool center areas might be explained by the contrasting thermal properties of the caliche material (duricrust) which is often deposited around these ponding areas. Another possible explanation would be that the slight increase in slope angle around the ponding areas may cause preferential solar heating as is the case with the fault scarps discussed below (refer to Figure 10, upper left hand corner, for close-up picture of the area discussed). Figures 8a and 8b are annotated and unannotated reproductions of a part of Line 33. The fault scarps are imaged relatively warm as a result of topographically controlled solar heating. The scarp faces are more nearly normal to the incoming solar energy than are the adjacent areas. Note the faint streaking oriented in a north-south direction. Because of ground control operations which monitored atmospheric conditions during the overflight, these features could confidently be attributed to wind effects.

Mission 105 radar imagery was of such poor quality as to be uninterpretable. Even large topographic features were difficult or impossible to identify.

Multifrequency microwave radiometer data were analyzed by Rosecrans (Lee, 1971, p. 51) who applied several enhancement techniques to the data. His conclusion was that no geologic, hydrologic, or topographic variation produced sufficient radiometric

differences to be detected above the noise level of the radiometers. It should be noted that the microwave system was not operating properly when the data were obtained.

RECENT SUPPLEMENTARY DATA--MISSION 168

Much valuable data were collected on Mission 168, which was flown during June 1971. Since these data arrived too late to be evaluated as part of this thesis, only a few highlights are discussed in this section. Table 5 summarizes the parameters of Mission 168 data that involve the thesis area.

The color and color IR photography of Mission 168 are generally superior to that produced by Mission 105. Although the scale of the Mission 168 photography is smaller, color balance, and stereo viewing geometry are superior to Mission 105 photography of the mountainous areas. Mission 105 photography of the San Luis Valley cannot be compared, since there is no comparable coverage by Mission 168 photography. Subtle color contrast between the Permian Pennsylvanian red beds and drab, gray-green sedimentary rocks could be detected and mapped in some areas. No new structural information was apparent. The color IR provided no significant advantage in Area 'C' by virtue of the film's near IR sensitivity. Similar lithologic color contrasts were noted as with the color photography. Both color and color IR portray gypsum and limestone outcrops much more prominently than these areas are portrayed on Mission 101 and Forest Service photography.

Table 5. Summary of Remote Sensing Instrument and Data Parameters--Mission 168

<u>Mode</u>	<u>System</u>	<u>Bandwidth</u>	<u>Format</u>	<u>(Approx.) Scale</u>	<u>Coverage</u>	<u>General Quality</u>
Photography (Color)	RC-8	400-700nm	9"x9" (P & T)	1:21,000	Area 'C', small part of 'B'	Very good (Hot Spots)
Photography (Color IR)	RC-8	500-900nm	9"x9" (T)	1:21,000	Area 'C', small part of 'B'	Very good (Hot Spots)
Photography (LSAP)	RC-8	590-900nm	9"x9" (P & T)	1:33,000	All of thesis area	Excellent but flown too early in eastern area
Thermal Scanner	RS-14	8-14 μ m	5" strip (P & T)	1:22,000	All of Area 'A', small part of Areas 'B' & 'C'	Good
SLAR	DPD-2	16.5 GHz	2" wide strips (T)	1:360,000	All of thesis area	Poor to fair

NOTE: A small amount of multiband photography was also flown over the thesis area. Since the film/filter combinations used were not designed for discriminating the rock types of the thesis area, this photography is not discussed. LSAP = low sun-angle photography.

Low sun-angle photography (LSAP), taken during the early morning with black and white infrared film, provides excellent enhancement of the fault scarps in the San Luis Valley (Figures 9a and 9b). Black and white infrared film was used with a Wratten 25 filter to make shadows (composed mostly of scattered blue light) darker and thus increase contrast. Note the decrease in enhancement between Figure 9a and Figure 9b. The photo frame from which Figure 9b was made was exposed only 16 minutes after that of Figure 9a. During this short interval, the sun had risen sufficiently to degrade the shadow enhancement noticeably. One of the primary objectives of obtaining the LSAP was to enhance the northwest trending lineaments of Area 'C' (Reeves, 1971, p. 18). This objective was not realized. Instead of emphasizing medium and small scale drainages, which are aligned to form the lineaments, only large scale drainages are enhanced. This problem was probably the result of both the high relief of this area and the somewhat lower than optimum angle of illumination. It is apparent that different types of terrain require separate study to establish the most advantageous angle of illumination for each terrain.

Only one channel (8-14 μ m) of thermal IR scan imagery is available for analysis. During the pre-dawn overflight of the scanner, radiometric and thermometric temperatures were

Reproduced from
best available copy.



Figure 9a. LSAP of fault scarps in San Luis Valley. Note shadow enhancement. Sun-angle is approximately 24° .

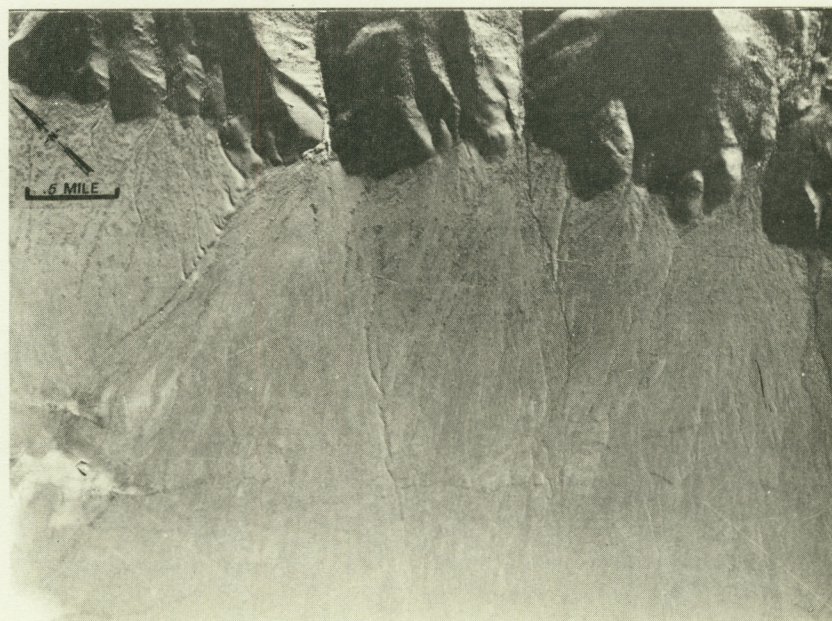


Figure 9b. LSAP of same general area as Figure 9a but taken approximately 16 minutes later. Note degradation of shadow enhancement. Sun-angle is approximately 27° .

measured across a fault scarp in the San Luis Valley (Figure 10). Stations were established on the upthrown side of the fault (1), on the fault scarp (2), and on the downthrown side of the fault (3). A similar distribution of stations was established in an area where ground water ponding occurs (stations designated 'W' for 'wet') and in an adjacent area, along the same fault scarp, where no ponding occurs (stations designated 'D' for 'dry'). Figure 10 is a close-up of a U. S. Forest Service photograph showing the location of the stations. At each 'W' station, thermometric temperatures were measured at depths of 0, 2.5, 5, 10, and 20cm. At each 'D' station, temperatures were measured at 0 and 5cm depths. In addition, surface soil samples and surface radiometric temperatures (using a Barnes PRT-5) were taken at each station. Atmospheric parameters were measured at a station located between the groups of 'W' and 'D' stations. Parameters that were measured include relative humidity, wind velocity, and air temperatures at 0, 25, 50, and 100cm above the ground. The surface and atmospheric data are presented in Table 6. These data suggest that evaporative cooling exerts a considerable control on relative surface temperatures. In general, radiometric temperatures are lower than corresponding thermometric temperatures, reflecting the fact that the ground surface is not a black body emitter. The imagery (Figure 11) indicates that the scanner may have a sensitivity of less than 1°C. In the area of the 'dry'

Reproduced from
best available copy.

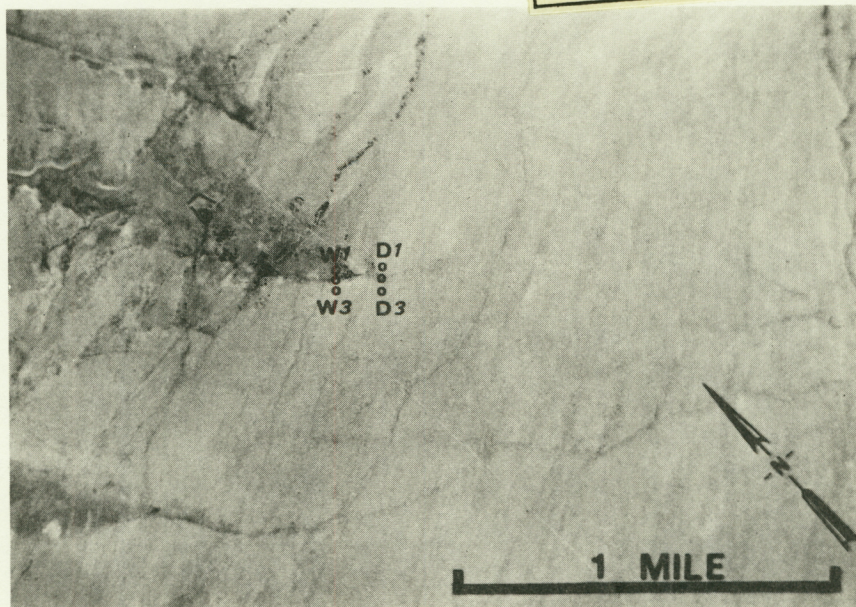


Figure 10. Close-up of Forest Service photograph showing location of temperature monitoring stations.

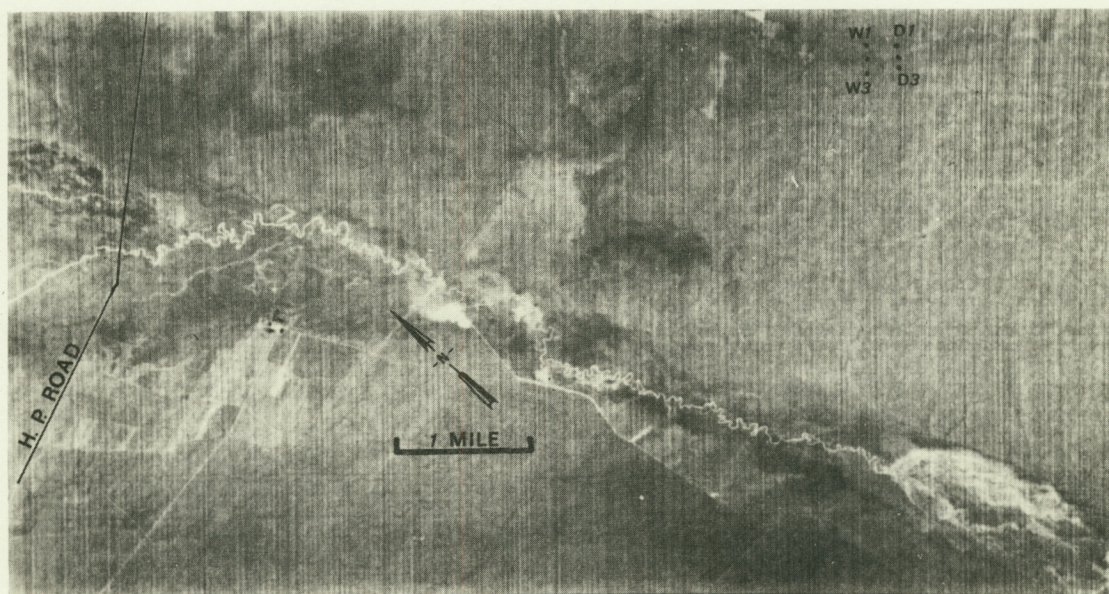
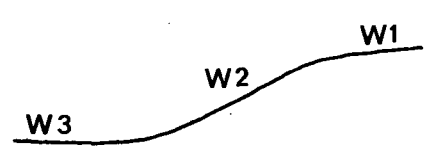
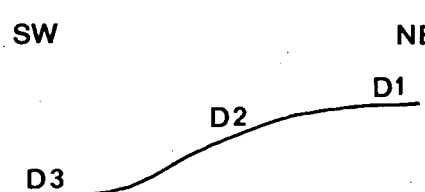


Figure 11. Reproduction of Mission 168 thermal IR imagery. Location of Hayden Pass Road and temperature monitoring stations shown. Imagery was obtained with an RS-14 in the 8-14 μ m bandwidth at 0500 hours on June 16, 1971.

Table 6. Measurements on Fault Scarps in San Luis Valley,
June 16, 1971

<u>Surface Data</u>				<u>Diagrammatic Profile</u>
<u>Station</u>	<u>Surf.Temp. Thermomet.</u>	<u>Surf.Temp. Radiomet.</u>	<u>Soil Moisture</u>	
W (1)	2.3°C	2°C	2.56%	
W (2)	1.0°C	1°C	3.52%	
W (3)	3.2°C	4°C	1.99%	
D (1)	4.3°C	4°C	1.12%	
D (2)	4.6°C	4°C	1.76%	
D (3)	5.0°C	4°C	1.18%	

Atmospheric Data

<u>Air Temperature</u>		<u>Relative Humidity</u>	<u>Wind</u>
<u>Above Ground</u>	<u>Temp.</u>		
0	2.1°C	(Dry = 43°F; Wet = 39°F) 72%	Calm; occasional light breeze from Sangre de Cristo Mountains.
25	4.7°C		
50	5.3°C		
100	5.9°C		

NOTE: Aircraft was overhead from 0440 to 0510 hours. Data
are interpolated, where necessary, to this time range.

stations, the fault scarp appears relatively warm, which does not agree with the radiometric data. However, near the 'wet' stations the fault scarp is imaged relatively cool, which is consistent with surface data. Comparison between this pre-dawn imagery and Mission 105 daytime thermal imagery (Figure 8) indicates that considerably more thermal contrast is available during the day when solar heating selectively heats the scarps as a function of the slope geometry of the scarps.

The SLAR imagery of Mission 168 is superior to that of Mission 105 and the Convair 990 radar flight. However, resolution is still poor and the small scale makes it suitable only for a more generalized regional study.

CONCLUSIONS

Remote sensor data provided definite advantages in the geological evaluation of the Hayden Pass--Orient Mine area. Overall, considerable time was saved in mapping the area by applying remote sensing techniques. The geologic map resulting from the integration of remote sensor and field data is more accurate and complete than would be a map based solely on field data. In addition, a greater understanding of certain geological phenomena and the detection of geological features not previously recognized was possible by analysis of Missions 101 and 105 data.

The greatest time saving, by use of remote sensing, was

realized in Area 'A'. About 5 days of laboratory time were required to interpret the remote sensor data and transfer the interpretations to a base map. Three days were spent in the field spot-checking features of Area 'A' to confirm their identities and locations as interpreted from the remote sensor data. Except for the mud flow features (Qmf on Plate II and Figure 7a), the origin of which is not certain, the interpretations proved to be accurate. Instead of the 8 days required to map Area 'A' using remote sensing methods, the author estimates that approximately 14 days would be required to map these same 20 square miles by field methods alone.

Time savings for Area 'B' were marginal. At least 10 days were required to interpret the remote sensor data and transfer the interpretations to a base map. The complexity of the geology, the thick cover of conifers, and the poor stereo-viewing geometry of the Mission 105 photography all added to the time required for interpretation. Transferring the interpretations to the base map by using a variable scale projector was difficult because of the many scale changes needed to compensate for the high relief of Area 'B'. Ten days were required to field check Area 'B' and the author believes that more time could have been spent in the complex Steel Canyon area if additional time were available. The total of 20 days needed to map and field check Area 'B' compares

with about an equal number of days that would be required to map Area 'B' by field methods unaided by remote sensing.

In Area 'C', no significant time savings were realized by the use of remote sensing methods. This is due, in part, to the lack of remote sensor data available of this area, but more directly to the very dense cover of conifers.

Possibly more significant than the time savings made possible by using remote sensing, was the higher quality map, in terms of accuracy and completeness, that resulted from the use of remote sensor data. Based on field experience gained while spot-checking interpreted features of Area 'A', it was obvious that the alluvial fan relationships shown on Plates I and II probably would not have been recognized and, if recognized, would not have been considered as practical mapable units without remote sensor data. Many of the fault scarps in the San Luis Valley are so subtle that they would not be noticed in the field even if the presence of these features in the valley were known. In Area 'B', the Mission 105 color photography was very valuable in completing the geology between field checked control points. The color photography was also a great aid in directing field efforts to areas of complex structure or anomalous stratigraphic relationships. The northwest trending faults of Area 'C' were first detected on small-scale Mission 101 color and color IR photography. Without this photography to direct

field investigation to the specific areas of faulting, it is doubtful that all the faults would have been adequately mapped.

The method used in this thesis of evaluating a particular sensor, by comparison of a map prepared from interpretation of data from that sensor (i. e., Plate II) with a map prepared by both interpretation of remote sensor data and field data (i. e., Plate I), is beneficial but not definitive. In particular, the following factors were detrimental to a meaningful evaluation of remote sensors as applied to the thesis area:

1. Sensor data were not of consistent quality throughout the area of coverage.
2. The data were generally not of the best quality possible from the various remote sensors.
3. Complete coverage of the thesis area was not obtained by all sensors.
4. The method implies that the map supported by field data (i. e., Plate I) is correct and complete when in fact the field map is also based largely on interpretation. This is particularly true in parts of Areas 'B' and 'C'.

In addition, a more meaningful evaluation of a particular sensor could have been made if the amount of time spent interpreting the data and the amount of time spent field mapping were accurately recorded. Only general estimates can now be made for the amount of time allocated to these tasks.

The following conclusions can be made regarding the various sensor modes:

1. Color and color IR RC-8 photography provided the largest amount of valuable information. The two film types must be rated about equal in effectiveness (based on comparison of small scale Mission 101 photography and medium scale Mission 168 photography). This statement applies to the thesis area only, as previous experience has indicated that one film type may be definitely superior to the other in certain terrains. Both large and small scale photography provided valuable information and both types serve a function in the geological analysis of an area. Small scale photography provides an overall view of regional and large scale structures, and gross lithologies. It also serves to direct attention to anomalous areas deserving more study (e. g., structurally controlled ponding in the San Luis Valley). Large scale photography provides the resolution necessary to do detailed geologic mapping. The superior resolution and overall excellent quality of the Zeiss photography should be used to better advantage. Future mission planning should provide for acquisition of stereo Zeiss photography of intermediate scale for further evaluation.

2. Multiband photography was of lesser value, since the information it provided was already available on the color and color IR photography. The multiband photography would be much more competitive with the RC-8 color and color IR

photography if it were designed specifically for the rocks in the area, based on field-measured reflectance spectra, were at the same scale, and had sufficient overlap for stereo viewing. Also, multiband photography must be in register so that various enhancement techniques may be applied to the data.

3. The thermal scanner imagery proved its ability to delineate much of the faulting in the San Luis Valley, but not nearly as well as the large scale photography could. In the mountainous areas, the main control on the thermal imagery was vegetation (tree covered versus open) and topography. Direct control on surface temperatures by surface moisture content or thermal properties of rocks was not apparent. In the San Luis Valley, thermal contrast across the fault scarps is greatest during the day when solar heating is influenced by slope geometry. Pre-dawn conditions provided thermal contrasts which were of marginal magnitude to be detected by the RS-14 scanner system. Pre-dawn surface temperatures are strongly affected by soil moisture differences related to the ground water impedance along fault planes. Thermal imagery is a very specialized remote sensing tool. It can be applied most gainfully to areas of low relief and sparse vegetation that have known or suspected surface thermal contrasts. This thermal contrast can and should be established by surface temperature monitoring before data from this sensor are requested.

4. The SLAR imagery produced no useable information that was not available on small-scale photography. Although

the radar imagery that was analyzed was not of adequate quality for meaningful evaluation, some generalizations can be made. SLAR imagery is necessarily of relatively small scale and always of lesser resolution than photography of similar scale. This sensor is best suited to more generalized studies where regional structure and gross lithologic discrimination are of interest.

5. Low sun-angle photography may offer a less expensive and higher resolution alternative to SLAR imagery. In areas of contrasting relief, such as the Hayden Pass--Orient Mine area, each type of terrain must be analyzed separately in order to determine the optimum illumination-angle. In general, terrains of high relief should be photographed at higher illumination-angles than low relief terrains.

BIBLIOGRAPHY

- Atwood, W. W., and Mather, K. F., 1924, Physiographic history of the San Luis Valley of Colorado and New Mexico (abs.): Geol. Soc. Amer. Bull., Vol. 35, no. 1, p. 121-123.
- Berg, R. R., 1962, Mountain flank thrusting in Rocky Mountain foreland, Wyoming and Colorado: Am. Assoc. Petroleum Geologists Bull., v. 46, no. 11, p. 2019-2032.
- Berg, T. M., 1967, Pennsylvanian biohermal limestones of Marble Mountain, south-central Colorado: Unpublished M.Sc. thesis, Univ. of Colorado.
- Blackwelder, E., 1928, The recognition of fault scarps: Jour. Geol., v. 36, p. 289-311.
- Bolyard, D. W., 1956, Pennsylvanian and Permian stratigraphy in the Sangre de Cristo Mountains between La Veta Pass and Westcliffe, Colorado: Unpublished M.Sc. thesis, Univ. of Colorado.
- 1959, Pennsylvanian and Permian stratigraphy in Sangre de Cristo Mountains between La Veta Pass and Westcliffe, Colorado: Am. Assoc. Petroleum Geologists Bull., v. 43, p. 1896-1936.
- 1960, Permo-Pennsylvanian stratigraphy in the Sangre de Cristo Mountains, Colorado: Geol. Soc. America, Guide to the Geology of Colorado, p. 121-126.
- Bridwell, R. J., 1968, The geology of the Kerber Creek area, Saguache County, Colorado: Unpublished M.Sc. thesis, Colo. School Mines, 104 p.
- Briggs, L. I., and Goddard, E. N., 1956, Geology of Huerfano Park, Colo.: Rocky Mtn. Assoc. Geo., Guidebook to the Geology of the Raton Basin, p. 40-45.
- Brill, K. G., 1952, Stratigraphy of the Permo-Pennsylvanian zeugogeosyncline of Colorado and northern New Mexico: Geol. Soc. America Bull., v. 63, p. 809-880.

- Burbank, W. S., 1933, Relationship of Paleozoic and Mesozoic sedimentation to Cretaceous-Tertiary igneous activity and the development of tectonic features in Colorado; in Ore Deposits of the Western States (Lindgren volume): Am. Inst. Min. Metall. Engineers, p. 277-301.
- Burbank, W. S., and Goddard, E. N., 1937, Thrusting in Huerfano Park, Colorado, and related problems of orogeny in the Sangre de Cristo Mountains: Geol. Soc. America Bull., v. 48, p. 931-976.
- Butler, C. R., 1949, Geology of the northern part of the Sangre de Cristo Mountains, Colorado (abs.): Geol. Soc. America Bull., v. 60, no. 12, pt. 2, p. 1959-1960.
- Chapin, C. E., 1971, The Rio Grande rift, Part I: modifications and additions, in New Mexico Geol. Soc. Guide-Book: 22d Field Conf., Oct., 1971, p. 191-201.
- Chronic, John, 1958, Pennsylvanian rocks in central Colorado, in Symposium on Pennsylvanian Rocks of Colorado and Adjacent Areas: Rocky Mtn. Assoc. of Geologists, p. 59-63.
- Costello, D. F., 1954, Vegetation zones in Colorado, in Harrington, H. D., Manual of the Plants of Colorado, Sage Books, Denver, p. iii-x.
- Curtis, B. F., 1958, Pennsylvanian paleotectonics of Colorado and adjacent areas, in Symposium on Pennsylvanian Rocks in Colorado and Adjacent Areas: Rocky Mtn. Assoc. Geol.
- Davis, W. M., 1913, Nomenclature of surface forms on faulted structures: Geol. Soc. America Bull., v. 24, p. 187-216.
- Dennis, J. C., (ed.), 1967, International tectonic dictionary: Am. Assoc. Petroleum Geologists Mem. 7, 196 p.
- De Voto, R. H., 1961, Geology of southwestern South Park, Park and Chaffee Counties, Colorado: Unpublished D.Sc. Thesis, Colo. School Mines, 323 p.
- _____, 1965, Pennsylvanian and Permian stratigraphy of central Colorado: The Mountain Geologist, v. 2, no. 4, p. 209-228.
- _____, 1968, Permo-Pennsylvanian block faulting and folding and the sedimentary record, central Colorado (abs.), in Geol. Soc. America Rocky Mountain Section program, p. 32.
- _____, 1971, Geologic history of South Park and geology of the Antero Reservoir quadrangle, Colorado: Colorado School Mines Quart., v. 66, no. 3, 90 p.
- _____, 1972, Permo-Pennsylvanian stratigraphy and tectonism of central Colorado: Colorado School Mines Quart., v. 67, no. 3, (in press).

- De Voto, R. H., Peel, F. A., and Pierce, W. H., 1971, Pennsylvanian and Permian stratigraphy, tectonism, and history, northern Sangre de Cristo Range, Colorado, in New Mexico Geol. Soc. Guidebook: 22nd Field Conf., Oct., 1971, p. 141-163.
- Endlich, F. M., 1874, Report on the mining districts of Colorado and on the geology of the San Luis district: U. S. Geol. Survey of Colo. and Adjacent territories (Hayden), Annual Report 7, p. 275-301, 305-361.
- Epis, R. C. (ed.), 1968, Cenozoic volcanism in the southern Rocky Mountains: Colo. School Mines Quart., v. 63, no. 3, 287 p.
- Gabelman, J. W., 1952, Structure and origin of northern Sangre de Cristo Range, Colorado: Am. Assoc. Petroleum Geologists Bull., v. 36, p. 1574-1612.
- _____, 1956, Tectonic history of the Raton Basin region: Rocky Mtn. Assoc. Geol., Guidebook to the Geology of the Raton Basin, Colorado, p. 35-39.
- Gaca, J. R., 1965, Gravity studies in the San Luis Valley area, Colorado: Unpublished M.Sc. Thesis, Colo. School Mines, 73 p.
- Gaca, J. R. and Karig, D. E., 1966, Gravity survey in the San Luis Valley area, Colorado: U. S. Geol. Survey open-file report, 21 p., 22-p app.
- Grose, L. T., 1972, Tectonics of the Rocky Mountain region: Geologic Atlas of the Rocky Mountain Region, Rocky Mountain Association of Geologists (in press).
- Hamilton, W. and Myers, W., 1966, Cenozoic tectonics of the Western U. S.: Rev. Geophysics, v. 4, p. 509-549.
- Hatfield, L. E., 1956, Stratigraphy of the Jacque Mountain and Whiskey Creek Pass Formations: M.Sc. Thesis, Unpublished, Univ. of Colorado, 99 p.
- Haun, J. D. and Weimer, R. J., 1960, Cretaceous stratigraphy of Colorado: Geol. Soc. America, Guide to the Geology of Colorado, p. 58-65.
- Haun, J. D., and Kent, H. C., 1965, Geologic history of Rocky Mountain region: Am. Assoc. Petroleum Geologists Bull., v. 49, no. 11, p. 1781-1800.
- Heard, H. and Rubey, W., 1966, Tectonic implications of gypsum dehydration: Geol. Soc. America Bull., v. 77, p. 741-760.

- Johnson, J. H., 1929, Contribution to the geology of the Sangre de Cristo Mountains of Colorado: Colo. Scientific Soc. Proc., v. 12, p. 1-21.
- _____, 1945, A resume of the Paleozoic stratigraphy of Colorado: Colo. School Mines Quart., v. 40, p. 1-109.
- Karig, D. E., 1964, Structural analysis of the Sangre de Cristo Range, Venable Peak to Crestone Peak, Custer and Saguache Counties, Colorado: Unpublished M.Sc. Thesis, Colo. School Mines, 143 p.
- Knepper, D. H., 1972, Tectonic evolution of the Rio Grande rift zone, central Colorado: an application of remote sensing to regional tectonic analysis: D.Sc. Thesis (in progress), Colo. School Mines.
- Koch, R. W., 1964, Geology of the Venable Peak area, Sangre de Cristo Mountains: Geol. Soc. America Bull., v. 69, p. 1143-1178
- Lee, Keenan, compiler, 1970, First annual report, NASA Grant NGL06-001-015: Dept. of Geology, Colo. School Mines.
- _____, compiler, 1971, NASA Mission 105 Summary report, NASA Grant NGL06-001-015: Dept. of Geology, Colo. School Mines.
- Litsey, L. R., 1954, Geology of the Hayden Pass--Orient area, Sangre de Cristo Mountains, Colorado: Unpublished Ph.D. dissertation, Univ. of Colorado.
- _____, 1956, Paleozoic stratigraphy of the northern Sangre de Cristo Range, Colorado, in Rocky Mtn. Assoc. Geologists Guidebook: p. 46-49.
- _____, 1958, Stratigraphy and structure of the northern Sangre de Cristo Mountains, Colorado: Geol. Soc. America Bull., v. 69, p. 1143-1178.
- _____, 1960, Geology near Orient Mine, Sangre de Cristo Mountains, Colorado, in Guide to the Geology of Colorado: Geol. Soc. America, Rocky Mtn. Assoc. Geologists, Colo. Sci. Soc., p. 129-131.
- Mallory, W. W., 1958, Pennsylvanian coarse arkosic redbeds and associated mountains in Colorado, in Symposium on Pennsylvanian rocks in Colorado and Adjacent Areas: Rocky Mtn. Assoc. Geologists, p. 17-29.
- _____, 1960, Outline of Pennsylvanian stratigraphy of Colorado, in Guide to the Geology of Colorado: Geol. Soc. America, p. 23-33.

- Mallory, 1965, Structural geology of the Spread Eagle Peak area, Sangre de Cristo Mountains, Colorado: The Mountain Geologist, v. 2, no. 1, p. 3-21.
- Munger, R. D., 1959, Geology of the Spread Eagle Peak area, Sangre de Cristo Mountains, Colorado: Unpublished M.Sc. Thesis, Univ. of Colorado.
- NASA, 1970, Screening and indexing report, Mission 101: Earth Resources Aircraft Program.
- _____, 1970, Screening and indexing report, Mission 105: Earth Resources Program.
- Nicolaysen, G. G., 1971, Geology of the Coal Dale area, Fremont County, Colorado: Unpublished M.Sc. Thesis, Colo. School Mines.
- Nolting, R. M., 1970, Pennsylvania-Permian stratigraphy and structural geology of the Orient--Cotton Creek area, Sangre de Cristo Mountains, Colorado: Unpublished M.Sc. Thesis, Colo. School Mines.
- Oriel, S. S. and Craig, L. C., 1960, Lower Mesozoic rocks in Colorado, in Guide to the Geology of Colorado: Geol. Soc. America, p. 43-58.
- Peel, F. A., 1971, New interpretations of Pennsylvanian and Permian stratigraphy and structural history, northern Sangre de Cristo Range, Colorado: Unpublished M.Sc. Thesis, Colorado School Mines.
- Peel, F. A. and De Voto, R. H., 1972, Pennsylvanian and Permian stratigraphy and structural history of northern Sangre de Cristo Range, Colorado: Colorado School Mines Quart., v. 67, no. 3 (in press).
- Pierce, W. H., 1967, Angular unconformity within Permo-Pennsylvanian strata near Howard, Colorado (abs.), in Geol. Soc. America Rocky Mountain Section program: p. 59-60.
- _____, 1969, Geology and Pennsylvanian-Permian stratigraphy of Howard area, Fremont County, Colorado: Unpublished M.Sc. Thesis, Colo. School Mines, 136 p.
- Powell, W. J., 1958, Ground-water resources of the San Luis Valley, Colorado: U. S. Geol. Survey Water-Supply Paper 1379, 284 p.

- Powers, W. E., 1935, Physiographic history of the upper Arkansas River Valley and the Royal Gorge, Colorado: Jour. Geol., v. 43, p. 184-199.
- Prucha, J. J., Graham, J. A., and Nickelsen, R. P., 1965, Basement-controlled deformation in Wyoming province of Rocky Mountains foreland: Am. Assoc. Petroleum Geologists Bull., v. 49, no. 7, p. 966-992.
- Rahman, Yousuf H., 1954, Geology of the Wellsville-Calcite area, Chaffee and Fremont Counties, Colorado: Unpublished D.Sc. dissertation, Colo. School Mines.
- Reeves, R. G., compiler, 1971, Semiannual progress report, NASA Grant NGL06-001-015: Dept. of Geology, Colo. School Mines.
- Richmond, G. M., 1960, Glaciation of the east slope of Rocky Mountain National Park, Colorado: Bull, G.S.A., v. 71, p. 1371-1382.
- Scott, G. R., 1953, Quaternary geology and geomorphic history of the Kassler Quadrangle, Colorado: U. S. Geol. Survey Prof. Paper 421-A, 70 p.
- _____, 1967, General and engineering geology of the United States Air Force Academy Site, Colorado, U.S. Geol. Survey Prof. Paper 551, 93 p.
- _____, 1970a, Quaternary faulting and potential earthquakes in east-central Colorado: U. S. Geol. Survey Prof. Paper 700-C, p. C11-C18.
- _____, 1970b, Geomorphic evolution of the southern Front Range, Colorado: Colorado Sci. Soc. unpublished Presidential Address, Dec. 21, 1970.
- Siebenthal, C. E., 1907, Notes on glaciation in the Sangre de Cristo Range: Jour. Geol., v. 15, p. 15-22.
- _____, 1910, Geology and water resources of the San Luis Valley, Colorado; U. S. Geol. Survey Water Supply Paper 240, 128 p.
- Silver, B. A., and Todd, R. G., 1969, Permian cyclic strata, northern Midland and Delaware Basins, West Texas and southeastern New Mexico: AAPG Bull., v. 53, no. 11, p. 2223-2251.

- Steven, T. A., and Epis, R. C., 1968, Ologocene volcanism in south-central Colorado: Colo. School Mines Quart., v. 63, p. 241-258.
- Stone, J. B., 1934, Limonite deposits at the Orient Mine, Colorado: Econ. Geology, v. 29, no. 4, p. 317-329.
- Stose, G. W., (ed.), 1935, Geologic map of Colorado: U. S. Geol. Survey Map.
- Toulmin, P. III, 1953, Petrography and petrology of Rito Alto Stock, Custer and Saguache Counties, Colorado: Unpublished M.Sc. Thesis, Univ. of Colorado.
- Tweto, Ogden, 1958, Pennsylvanian stratigraphic section in the Minturn-Pando area, Colorado, in Symposium on Pennsylvanian Rocks of Colorado and Adjacent Areas: Rocky Mountain Assoc. Geologists.
- Van Alstine, R. E., 1968, Tertiary trough between the Arkansas and San Luis Valleys, Colorado: U. S. Geol. Survey Prof. Paper 600-C, p. C158-C160.
- Van Alstine, R. E., and Lewis, G. E., 1960, Pliocene sediments near Salida, Chaffee County, Colorado: U. S. Geol. Survey Prof. Paper 400-B, p. B245.
- Van Andel, T. H., 1963, Recent marine sediments of Gulf of California, in Marine Geology of the Gulf of California, a Symposium: Am. Assoc. Petroleum Geologists, Memoir 3, p. 216-310.
- Vargus, D. F., 1960, Geology of the Cotopaxi inlier on the northern end of the Sangre de Cristo Range, Fremont County, Colorado: Unpublished M.Sc. Thesis, Colo. School Mines.
- Walker, T. R., 1967, Formation of redbeds in modern and ancient deserts: Geol. Soc. America Bull., v. 78, p. 353-368.
- Wychgram, D. C., 1972, Geology of the Hayden Pass--Orient Mine area, northern Sangre de Cristo Mountains, Colorado: a geologic remote sensing evaluation: Unpublished M.Sc. Thesis, Colo. School of Mines.

DISTRIBUTION

Copies

NASA - HEADQUARTERS

Molloy, M. J.	1
Park, A. B.	1
Sci. & Tech. Information Facility	5
Vitale, J. A.	1

NASA - MSC

Amsbury, D.	1
MacDonald, R. B.	1
Newman, F.	1
Smistad, O.	1
Watkins, A.	1
Zeitler, E.	5

USGS

Canney, F. C.	1
Carter, W. D.	1
Fischer, W. A.	1
Hemphill, W. R.	1
Robinove, C. J.	1
Smedes, H. W.	1
Watson, K.	1

MMC

Muhm, J.	5
----------	---

OTHERS

Cole, B. L.	1
Danielson, J. A.	1
Joiner, T. J.	1
Lepley, L. K.	1
Lyon, R. J. P.	1
Meyers, V.	1
Paulton, C. E.	1
Quade, J.	1
Sabins, F. F.	1
Taranik, J. V.	1

Copies

CSM

Grose, L. T.	1
Jordan, A. R.	1
Kent, H. C.	1
Klodt, D. T.	1
Kuhn, T. H.	1
Lee, K.	1
McBride, G. T.	1
Reeves, R. G.	1
Weimer, R. J.	1
Bonanza Project	31